Electron pairing and Coulomb repulsion in one-dimensional anharmonic lattices

L. Brizhik,[1,2,3] A. P. Chetverikov,[2,4] W. Ebeling,[2,5] G. Röpke,[2,6] and M. G. Velarde[2,3]
[1]*Bogolyubov Institute for Theoretical Physics, Metrolohichna Str., 14b, Kyiv 03680, Ukraine*
[2]*Instituto Pluridisciplinar, Universidad Complutense, Paseo Juan XXIII, 1, Madrid 28040, Spain*
[3]*Wessex Institute of Technology, Ashurst, Southampton SO40 7AA, United Kingdom*
[4]*Faculty of Physics, Chernyshevsky State University, Astrakhanskaya b. 83, Saratov 410012, Russia*
[5]*Institut für Physik, Humboldt Universität, Newtonstrasse 15, Berlin 12489, Germany*
[6]*Institut für Physik, Universität Rostock, Rostock 18051, Germany*
(Received 1 March 2012; published 6 June 2012)

We show that in anharmonic one-dimensional crystal lattices pairing of electrons or holes in a localized *bisolectron* state is possible due to the coupling between the charges and the lattice deformation that can overcome the Coulomb repulsion. Such localized states appear as traveling ground *singlet* states of two extra electrons bound in the potential well created by the local lattice solitonlike deformation. We also find the first excited localized state of two electrons given by a *triplet* state of two electrons. The results of the analytical study of interacting electrons in a lattice with *cubic* anharmonicity are compared with the numerical simulations of two electrons in an anharmonic lattice with Morse interactions and taking into account the single-site Hubbard electron-electron repulsion. We find quite a good qualitative agreement between both approaches for a broad range of parameter values. For illustration we give expressions for the bisolectron binding energy with parameter values that are typical for biological macromolecules. We also estimate threshold values of the Coulomb repulsion above which the bisolectron splits into two solectrons.

DOI: 10.1103/PhysRevB.85.245105 PACS number(s): 71.10.Li, 63.20.Ry, 71.38.Mx

I. INTRODUCTION

A broad class of low-dimensional systems such as polydiacetylene crystals,[1–4] conducting platinum chain compounds and conducting polymers,[5] salts of transition metals (PbSe, PbTe, PbS),[6–9] and superconducting cuprates[10–15] which find numerous applications in microelectronics and nanotechnologies, or play an important role in living systems (polypeptide macromolecules, DNA, etc.),[16–23] manifest nonlinear effects. These effects arise either from the electron-lattice interaction or from the (nonlinear) lattice *anharmonicity* and, eventually, from both items coupled together. As a consequence there is the formation of electro-solitons or solectrons which are bound states of an electron to a soliton[16,24] thus generalizing the polaron concept.[25–31] Furthermore, lattice anharmonicity can support the formation of two-component solitons.[32–34] Besides, pairing of two excess electrons or holes[35–43] may be enhanced bringing strong electron correlation both in *momentum* space and in *real* space.

The problem for pairing of charged particles is the Coulomb repulsion. In normal metallic superconductors, the attractive interaction needed to form a bound state of electrons (Cooper pair) is due to the retardation of the electron-phonon interaction in the *harmonic* lattice. Lattice polarization overcomes the Coulomb repulsion so that for states near to the Fermi surface, where the repulsion is rather weak, pairing becomes possible (in *momemtum* space only with complete delocalization in real space). This situation changes in the strong coupling case where the two-electron bound state is localized in space on one lattice site (small bipolaron).[28,29]

In particular, for one-dimensional electron-lattice systems with *cubic* or *quartic* anharmonicity, it has been shown[38,39] that two excess electrons with opposite spins may form a *bisolectron*, which is a localized bound state of the paired electrons in a lattice solitonlike deformation. When one *excess* electron is spread on several lattice sites forming a *solectron* state the Coulomb repulsion between two electrons in a bisolectron is not as strong as in a small bipolaron, but is not negligible as in the case of completely delocalized electrons.

In contrast to two- and three-dimensional systems, the Coulomb interaction can lead to divergent potential energy in one-dimensional systems if both electrons are found with finite density at the same point in space. This singularity can be removed by using the Hubbard (local) model of Coulomb interaction in a discrete lattice.[44,45] We consider in Sec. II the case when the electron-lattice interaction is moderately strong, so that an adiabatic approximation is valid in the continuum approximation. First we consider the *cubic* anharmonicity in the lattice interactions. We also take the Coulomb interaction weak enough, hence not modifying too much the two-electron bisolectron wave function (Sec. III). Subsequently, we consider the rather strong Coulomb repulsion case for which we find the two-electron wave function using a variational approach (Sec. IV). Solutions for the ground state and the first excited state are considered in Sec. V. In Sec. VI we compare these analytical results with numerical results of computer simulations in a lattice with interactions between nearest neighbors described by the Morse potential while the electrons are considered in the Hubbard (local interaction) model. The comparison of results, in so apparently drastically different approaches, shows quite a good qualitative agreement. Finally, in Sec. VII we draw some conclusions, discussing the applicability of the continuum model and the stability of the bisolectron state. All through the work we have used parameter values corresponding to biological macromolecules.

II. DYNAMICS OF THE COUPLED ELECTRON-LATTICE SYSTEM

We consider an infinitely long, one-dimensional (1D) crystal lattice, with units all of equal mass M and equilibrium lattice spacing a, where two free, excess electrons are added. The Hamiltonian of such a system can be represented in the form:

$$\hat{H} = \hat{H}_{\rm el} + \hat{H}_{\rm lat} + \hat{H}_{\rm int} + \hat{H}_{\rm Coul}. \tag{1}$$

Let E_0 denote the onsite electron energy, let J denote the electron exchange interaction energy, and let $\hat{c}^{\dagger}_{n,s}$ and $\hat{c}_{n,s}$ be the creation and annihilation operators of an electron with the spin projection $s = \uparrow, \downarrow$ at the site n. Then the electron Hamiltonian (1) has the explicit form

$$\hat{H}_{\rm el} = \sum_{n,s}[E_0\hat{c}^{\dagger}_{n,s}\hat{c}_{n,s} - J\hat{c}^{\dagger}_{n,s}(\hat{c}_{n+1,s} + \hat{c}_{n-1,s})]. \tag{2}$$

Taking into account only longitudinal displacements of atoms from their equilibrium positions, the lattice part of the Hamiltonian (1) has the form

$$\hat{H}_{\rm lat} = \sum_{n}\left[\frac{\hat{p}_n^2}{2M} + \hat{U}_{\rm lat}(\hat{u}_n)\right], \tag{3}$$

where $\hat{u}_n$ is an operator of the nth atom displacement, $\hat{p}_n$ is the operator of the canonically conjugated momentum, and $\hat{U}_{\rm lat}$ is the operator of the lattice potential energy, whose properties will be specified below.

We consider the case when the dependence of the onsite electron energy on atom displacements is much stronger than that of the exchange interaction energy, so that the electron-lattice interaction part of the Hamiltonian (1) has the form

$$\hat{H}_{\rm int} = \chi\sum_{n,s}(\hat{u}_{n+1} - \hat{u}_{n-1})\hat{c}^{\dagger}_{n,s}\hat{c}_{n,s}, \tag{4}$$

where χ accounts for the strength of electron-lattice interaction. The Coulomb repulsion between the electrons is

$$\hat{H}_{\rm Coul} = \sum_{n,m,s,s'} U_{nm}\hat{c}^{\dagger}_{n,s}\hat{c}^{\dagger}_{m,s'}\hat{c}_{m,s'}\hat{c}_{n,s}, \tag{5}$$

where U_{nm} is the matrix element corresponding to the Coulomb interaction of electrons placed at sites n and m along the lattice.

In the Born-Oppenheimer approximation we can factorize the state vector of the system into two parts,

$$|\Psi(t)\rangle = |\Psi_{\rm el}(t)\rangle|\Psi_{\rm lat}(t)\rangle. \tag{6}$$

Here the state vector of the lattice has the form of the product of the operator of coherent displacements of the atoms and the vacuum state of the lattice

$$\begin{aligned} |\Psi_{\rm lat}(t)\rangle &= S(t)|0\rangle_{\rm lat}, \\ S(t) &= \exp\left\{-\frac{i}{\hbar}\sum_n[u_n(t)\hat{p}_n - p_n(t)\hat{u}_n]\right\}, \end{aligned} \tag{7}$$

where $u_n(t)$, $p_n(t)$ are, respectively, the mean values of the displacements of atoms from their equilibrium positions and their canonically conjugated momenta in the state (6).

In the case of two excess electrons with spins s_1,s_2 in the lattice, the electron state-vector has the form

$$|\Psi_{\rm el}(t)\rangle = \sum_{n_1,n_2,s_1,s_2}\Psi(n_1,n_2,s_1,s_2;t)\hat{c}^{\dagger}_{n_1,s_1}\hat{c}^{\dagger}_{n_2,s_2}|0\rangle_{\rm el}. \tag{8}$$

We use for the function $\Psi(n_1,n_2,s_1,s_2;t)$ the normalization condition

$$\sum_{n_1,n_2,s_1,s_2}|\Psi(n_1,n_2,s_1,s_2;t)|^2 = 1. \tag{9}$$

In the absence of magnetic field the electron wave function of the system can be represented by the product of the spatial and the spin wave functions. The antisymmetry requirement of the two-electron wave function may be fulfilled by the symmetry of the spatial wave function and the antisymmetry of the spin function (singlet state) or by the antisymmetry of the coordinate function and the symmetry of the spin wave function (triplet state). Using the state vector (6)–(8) we can calculate the Hamiltonian functional H, corresponding to the Hamiltonian operator (1):

$$H = \langle\Psi(t)|\hat{H}|\Psi(t)\rangle. \tag{10}$$

Minimizing the functional (10) with respect to electron and phonon variables, a system of two coupled equations for the two-electron wave function and the atom displacements can be derived. In the continuum approximation $n \to x \equiv na$ this system of equations is:

$$\begin{aligned} i\hbar\frac{\partial\Psi(x_1,x_2,t)}{\partial t} &= -\frac{\hbar^2}{2m}\left(\frac{\partial^2}{\partial x_1^2} + \frac{\partial^2}{\partial x_2^2}\right)\Psi(x_1,x_2,t) \\ &\quad + \chi a\left(\frac{\partial u(x,t)}{\partial x}\bigg|_{x=x_1} + \frac{\partial u(x,t)}{\partial x}\bigg|_{x=x_2}\right)\Psi(x_1,x_2,t) \\ &\quad + U_{\rm Coul}(x_1,x_2)\Psi(x_1,x_2,t), \end{aligned} \tag{11}$$

$$\begin{aligned} \frac{\partial^2 u}{\partial t^2} - V_{\rm ac}^2\frac{\partial^2 U_{\rm lat}}{\partial\rho^2}\frac{\partial^2 u}{\partial x^2} &= \frac{a}{M}\chi\left(\frac{\partial}{\partial x_1}\int dx_2|\Psi(x_1,x_2,t)|^2|_{x_1=x}\right. \\ &\quad \left. + \frac{\partial}{\partial x_2}\int dx_1|\Psi(x_1,x_2,t)|^2|_{x_2=x}\right). \end{aligned} \tag{12}$$

Here, $V_{\rm ac} = a\sqrt{w/M}$ is the sound velocity in the lattice. w is the lattice elasticity coefficient, defined by the Young modulus $E = wa$. The sound velocity in the chain coinciding with the phase velocity of acoustic phonons from the dispersion is $\omega^2(k) = (4w/M)\sin^2(ka/2)$ in the long-wavelength limit $ka \ll 1$. $\Psi(x_1,x_2,t)$ is the two-electron spatial wave function with $x_i = n_i a$, $i = 1,2$, $u(x,t)$ is the function of the lattice displacement, and $U_{\rm Coul}$ accounts for the Coulomb repulsion between the two electrons. Note that to study the case of strong electron localization we ought to augment equation (12) with an additional term $\propto\partial^4 u/\partial x^4$ which takes into account the dispersion of the lattice and can lead to supersonic solutions, see, e.g., Ref. 46. Such a possibility would be considered elsewhere.

Introducing the function of the lattice deformation

$$\rho(x,t) = -\frac{\partial u(x,t)}{\partial x}, \tag{13}$$

we can write the potential energy of the system appearing in the right hand side of the Schrödinger equation (11) in the form

$$U_{\rm tot} = U_{\rm sol}(x_1,x_2,t) + U_{\rm Coul}(x_1,x_2), \tag{14}$$

$$U_{\rm sol}(x_1,x_2,t) = -\chi a[\rho(x_1,t) + \rho(x_2,t)], \tag{15}$$

where the function $U_{\rm sol}(x_1,x_2,t)$ plays the role of an effective potential created by the deformation of the lattice (index "sol" indicates that this potential is solitonlike, as will be shown below).

In lowest order, for the case of a lattice with *cubic* anharmonicity the potential energy of the lattice, measured in units of wa^2, is

$$U_{\rm lat}(\rho) = \frac{1}{2}\rho^2 + \frac{\gamma}{3}\rho^3, \tag{16}$$

where γ is the anharmonicity parameter whose value is positive, as we wish to focus on strong enough compressions for which the repulsion part of the potential is what really matters.

The solution of Eqs. (11) and (12) for the singlet two-electron problem without the Coulomb repulsion, i.e., when in Eq. (11) $U_{\rm Coul}$ is omitted, was found previously.[38] In particular, it was found that the lattice deformation is given by the expression

$$\rho(\xi) = \rho_0 {\rm sech}^2(\kappa\xi), \quad \xi = (x - Vt)/a, \tag{17}$$

with

$$\kappa = \frac{1}{2}\sqrt{\sigma\rho_0}, \quad \sigma = \frac{\chi a}{J}. \tag{18}$$

The maximum value of the lattice deformation ρ_0 depends on the soliton velocity V and lattice anharmonicity γ. In the moving frame, $V = 0$, it is approximately

$$\rho_0(V=0) \approx \frac{1}{2}\alpha^2\gamma^2\left[1 + \frac{3}{144}\alpha^2\gamma^3\right], \tag{19}$$

with

$$\alpha = \frac{2\delta}{\gamma}\sqrt{\sigma}, \quad \delta = \frac{\chi a}{MV_{\rm ac}^2} = \frac{\chi}{aw}. \tag{20}$$

In the laboratory frame, for arbitrary values V of the velocity, $\rho_0(V)$ can be obtained numerically.

The solution for the singlet two-electron wave function is

$$\Psi(x_1,x_2,t) = \tfrac{1}{2}[\Psi_1(x_1,t)\Psi_2(x_2,t) + \Psi_2(x_1,t)\Psi_1(x_2,t)]. \tag{21}$$

The single-electron wave functions $\Psi_1(x,t) = \Psi_2(x,t) \equiv \Psi(x,t)$ are normalized to 1, according to Eq. (9). The modulus $|\Psi(x,t)| \equiv \Phi(\xi)$ is found to be of the soliton-type form,

$$\Phi(\xi) = \sqrt{\frac{\rho_0}{2\delta}}{\rm sech}(\kappa\xi)\sqrt{1 - s^2 + \gamma\rho_0{\rm sech}^2(\kappa\xi)}, \tag{22}$$

with $s^2 = V^2/V_{\rm ac}^2$. The phase factor contains the energy. Clearly, the parameter κ in Eqs. (17) and (22) determines the width of electron localization in the bisolectron state (22) yet without Coulomb repulsion. The binding energy has been found:

$$\begin{aligned} E^{\rm (bind)} &= 2E^{\rm (sol)}(V) - E^{\rm (bis)}(V) \\ &= \chi a\left[\rho_0\frac{\frac{4}{3}\gamma\rho_0 + 1 - s^2}{\gamma\rho_0 + 1 - s^2} - \rho_0^{\rm (sol)}\frac{\frac{4}{3}\gamma\rho_0^{\rm (sol)} + 1 - s^2}{\gamma\rho_0^{\rm (sol)} + 1 - s^2}\right] > 0. \end{aligned} \tag{23}$$

Here, $E^{\rm (sol)}$ and $\rho_0^{\rm (sol)}$ are the energy and maximum lattice deformation for the solectron state where a single electron is bound to the lattice soliton. Typical values for biological macromolecules like polypeptides[17] are: $\chi = 35 - 62$ pN, $a = 5.4 \cdot 10^{-10}$ m, $w = 39 - 58$ N/m, $M = 5.7 \cdot 10^{-25}$ kg, and $V_{\rm ac} = (3.6 - 4.5) \cdot 10^3$ m/s. The transfer energy value for the amid-I excitation is $J_{\rm exc} = 0.001$ eV, and the electron transfer energy is of the order $J \approx 0.1$–0.5 eV. For these parameter values, the bisolectron binding energy (23) in macromolecules is in the range $E^{\rm (bind)} \approx 0.05$–$0.5$ eV, if the Coulomb repulsion is neglected.

III. LIMIT CASE OF WEAK COULOMB REPULSION

If the bisolectron state is extended over few lattice sites, i.e., if the width of the bisolectron $l^{\rm (bis)}a = 2\pi a/\kappa$ is bigger than a, the Coulomb repulsion is rather weak relative to the binding energy of the bisolectron (23). Therefore, the wave function (22) can be generalized as (see Refs. 35, 36, and 39)

$$\begin{aligned} \Phi_{1,2}(\xi) = &\sqrt{\frac{\rho_0}{2\delta}}{\rm sech}[\kappa(\xi \mp l/2)] \\ &\times\sqrt{1 - s^2 + \gamma\rho_0{\rm sech}^2[\kappa(\xi \mp l/2)]}. \end{aligned} \tag{24}$$

Here the parameter l recalls the Coulomb repulsion in Eq. (11). To a first approximation

$$U_{\rm Coul} = \frac{e^2}{4\pi\epsilon la}, \tag{25}$$

and hence l provides an estimate of the distance between the center of mass (c.o.m.) coordinates of one-electron wave functions. ϵ denotes the dielectric constant of the lattice and in SI units $\epsilon = \epsilon_{\rm rel}\epsilon_0$ contains the relative dielectric constant $\epsilon_{\rm rel}$ of the system.

The parameter l can be determined from the condition of the minimum of energy. Averaging the energy functional (10) with the two-electron wave function (21) using the state functions (24), we obtain for the total energy of the system

$$\begin{aligned} E^{\rm (bis)} = &2E_0 + \frac{2}{3}J\kappa^2\frac{\rho_0}{\delta} - \frac{4}{3}\frac{\chi a\rho_0^2}{\kappa\delta}(1 - l^2\kappa^2) \\ &+ wa^2\rho_0^2\left[\frac{2}{3} + \frac{1}{2}\gamma\rho_0^2 - l^2\kappa^2\left(\frac{1}{3} + \frac{1}{2}\gamma\rho_0^2\right)\right] \\ &+ \frac{e^2}{4\pi\epsilon la}. \end{aligned} \tag{26}$$

Minimizing this expression with respect to l, we get the equilibrium distance between the maxima of one-electron functions:

$$l_0 = \frac{1}{2}\left(\frac{e^2}{\pi\epsilon a\zeta}\right)^{1/3} \tag{27}$$

where

$$\zeta = \left[\frac{4}{3}\frac{\chi a\rho_0^2\kappa}{\delta} - wa^2\rho_0^2\kappa^2\left(\frac{1}{3}+\frac{1}{2}\gamma\rho_0^2\right)\right]. \quad (28)$$

Then (27) can be approximated by

$$l_0 = \frac{1}{2}\left(\frac{3\delta e^2}{4\pi\epsilon\chi a^2\rho_0^2\kappa}\right)^{1/3}. \quad (29)$$

Strictly speaking, this approach is valid when the distance between the two maxima is small compared to the width of the bisolectron wave function so that the condition $l_0 \ll l^{(\mathrm{bis})} = 2\pi/\kappa$ is fulfilled. Thus we find a lattice soliton binding two electrons together in the lattice deformation potential well (15). The bisolectron solution is stable when its binding energy is higher than the Coulomb repulsion and hence in view of Eq. (23) $Jg^2/2 > U_{\mathrm{Coul}}$, where $g = \chi^2/(2Jw)$. For polypeptides the value $g = (0.9\text{–}3.9)$ is found.[17] Therefore we conclude that the threshold or critical value of the electron-lattice coupling constant χ increases with increasing Coulomb repulsion in agreement with the results given in Ref. 47. Note that the Coulomb interaction is screened by the relative dielectric constant ϵ_{rel} of the order of 10. For the parameter values given above, we find that l_0 is small compared with $2\pi/\kappa$ so that the weak coupling condition holds. The estimation for the binding energy $E^{(\mathrm{bis})}$ gives a value of about 0.05 eV indicating a stable bisolectron solution, as expected.

In Sec. VI, Fig. 4, we will show the charge density distribution $q(\xi) = \Phi_1^2(\xi) + \Phi_2^2(\xi)$ for three different values of l_0, i.e., for three different values of the ratio between the binding energy of the bisolectron and the Coulomb repulsion strength (25). The density profile has one maximum at relatively small values of l_0 and two maxima at large values of l_0, indicating when the bisolectron splits into two solectrons.

IV. SEPARATION OF THE TWO-ELECTRON CENTER OF MASS MOTION

Let us consider the case of arbitrary Coulomb repulsion. The Coulomb term in Eq. (11) is represented as

$$U_{\mathrm{Coul}} = \frac{e^2}{4\pi\epsilon|x_1 - x_2|}. \quad (30)$$

Let the c.o.m. coordinate be $X = (x_1 + x_2)/2 - Vt$, the running wave coordinate of the soliton moving with velocity V, with relative coordinate $x = x_2 - x_1$. The interaction of the electrons with the lattice is described by the effective deformational potential (15). Let us assume that the solution for the soliton potential $U_{\mathrm{sol}}(x_1,x_2,t)$ can be represented in the form

$$\begin{aligned} U_{\mathrm{sol}}(x_1,x_2,t) &\approx U_{\mathrm{sol}}^{(0)}(x_1,x_2,t) = -\chi a[\rho^{(0)}(x_1,t) + \rho^{(0)}(x_2,t)] \\ &\approx -2\chi a\rho^{(0)}(X,t) + U_{\mathrm{rel}}(x,t;X), \end{aligned} \quad (31)$$

where the superscript (0) indicates solutions in the absence of the Coulomb interaction. Expanding $U_{\mathrm{rel}}(x,t;X)$ to second order with respect to x, we have

$$\begin{aligned} U_{\mathrm{rel}}(x,t;X) &\approx \frac{1}{2}m\omega_0^2x^2, \\ m\omega_0^2 &= -\frac{1}{2}\chi a\frac{\partial^2\rho^{(0)}(X,t)}{\partial X^2}\bigg|_{X=0} = \frac{\chi\rho_0\kappa^2}{a}. \end{aligned} \quad (32)$$

Since the potential (31) splits into two parts we may, accordingly, separate the Hamiltonian functional

$$\begin{aligned} H_{\mathrm{eff}} = &-\frac{\hbar^2}{4m}\frac{\partial^2}{\partial X^2} - \frac{\hbar^2}{m}\frac{\partial^2}{\partial x^2} \\ &- 2\chi a\rho^{(0)}(X,t) + \frac{1}{2}m\omega_0^2x^2 + \frac{e^2}{4\pi\epsilon|x|}. \end{aligned} \quad (33)$$

Here we have used only the first nonvanishing term of the expansion of the potential around its minimum. In general, the relative potential well in the co-moving coordinates $U_{\mathrm{rel}}(x,t;X)$ depends not only on the relative coordinate x but also on the center of mass position X so that the relative motion and the c.o.m. motion remain coupled.

Our aim was to separate the problem into a c.o.m. problem identical to the previous task without Coulomb repulsion and a parabolic problem for the relative motion. This way we have first to solve the soliton problem for the common motion to find the function $\rho^{(0)}(X,t)$ and ω_0, and then we solve the parabolic problem including the Coulomb term (30).

With the ansatz $\Psi(x_1,x_2,t) = \Phi(X)\phi(x)$, $E = E_{\mathrm{c.o.m.}} + E_{\mathrm{rel}}$, we get the equation for the center of mass motion

$$\left[-\frac{\hbar^2}{4ma^2}\frac{d^2}{d\xi^2} - 2\chi a\rho^{(0)}(\xi)\right]\Phi(a\xi) = E_{\mathrm{c.o.m.}}\Phi(a\xi). \quad (34)$$

where $\xi = X/a$. The soliton deformation $\rho^{(0)}(\xi)$ is obtained using Eq. (17). Therefore the soliton part of the deformation potential (31)

$$U_{\mathrm{sol}}(\xi) = -2\chi a\rho_0\mathrm{sech}^2(\kappa\xi). \quad (35)$$

Up to order ξ^2, (35) reduces to

$$U_{\mathrm{eff}}(\xi) = -2\chi a\rho_0 e^{-\kappa^2\xi^2}, \quad (36)$$

Fig. 1 illustrates the deformation potentials for the case $\gamma = 1.5$ and other parameters corresponding to their values in polypeptide macromolecules. The parabolic approximation (32) is possible only for $x \leqslant a/\kappa$. For larger distances, the deformation potential becomes too shallow.

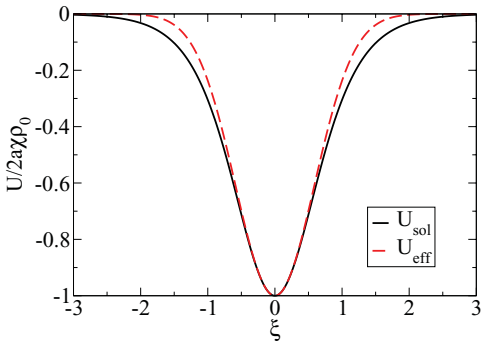

FIG. 1. (Color online) Deformation potential (35) for $\gamma = 1.5, \delta = 0.002$, $\rho_0 = 0.007$, and $\kappa = 1.2$, (black solid line) and the Gaussian (36) fitted to the region around the minimum (red dashed line). Potentials are given in units $2\chi a\rho_0$.

V. WAVE FUNCTION FOR THE TWO-ELECTRON RELATIVE MOTION INCLUDING COULOMB REPULSION

Let us now solve the Schrödinger equation for the relative motion of electrons:

$$\left(-\frac{\hbar^2}{m}\frac{d^2}{dx^2}+\frac{m\omega_0^2}{2}x^2+\frac{e^2}{4\pi\epsilon|x|}\right)\phi(x)=E_{\rm rel}\phi(x), \qquad (37)$$

with the symmetry condition for Fermions that in the spin singlet state $\phi(-x)=\phi(x)$ (symmetric orbital) and in the spin triplet state $\phi(-x)=-\phi(x)$ (antisymmetric orbital).

The minimum of the potential follows from Eq. (37) at $x=x_0$, where

$$x_0=\left(\frac{e^2}{4\pi\epsilon m\omega_0^2}\right)^{1/3} \qquad (38)$$

that may be considered as a characteristic length scale. In a classical treatment, it gives the distance between the two electrons at zero temperature.

In the absence of Coulomb repulsion, the solutions for the harmonic potential are Hermitian functions. The ground state is given by the symmetric orbital that has no nodes, but has a finite density at $x=0$ that thus leads to a divergent energy if Coulomb repulsion is considered. Therefore, taking into account Coulomb repulsion we have in the 1D case the additional condition $\phi(0)=0$ for strongly localized electrons, i.e., only solutions with a node at $x=0$ are possible. To consider the behavior near $x=0$, we have $\phi(x)\propto x+e^2m/(2\hbar^2\epsilon)x^2$. Therefore, both electrons are kept apart by a distance of the order x_0 (38). Comparing this expression with the result (27), it should be mentioned that now the deformation of the lattice remains fixed while the distance between the electrons varies.

A rigorous solution can be given in the free case $\omega_0=0$ using hypergeometric functions

$$\phi(x)=\text{const}x\exp[-i(mE_{\rm rel}/\hbar^2)^{1/2}x]\times{}_1F_1\left[1-i\frac{e^2}{4\pi\epsilon(E_{\rm rel}\hbar^2/m)^{1/2}},2,2i(mE_{\rm rel}/\hbar^2)^{1/2}x\right]. \qquad (39)$$

This solution approximates the full solution with the harmonic potential, $\omega_0\neq 0$, near $x=0$. As a peculiarity of the 1D Coulomb problem, symmetric solutions $\phi(-x)=\phi(x)$ and antisymmetric solutions $\phi(-x)=-\phi(x)$ become degenerated. This is an artifact of the continuum limit for strongly localized solutions. It disappears if we consider a discrete lattice and take into account the higher dimensionality of real systems (even so-called one-dimensional systems are in fact constrained three-dimensional systems).

In Ref. 38 we have reported the solution $\phi(x)$ of the Schrödinger equation for the relative motion obtained using a variational approach. In view of the above, we consider the normalized function

$$\phi_1(x;\beta)=2\left(\frac{2\beta^3}{\pi}\right)^{1/4}xe^{-\beta x^2} \qquad (40)$$

which is a Hermitian function for the first excited state. We can improve this ansatz using, e.g., higher Hermitian functions or other zero-node functions like $x\,\text{sech}(\beta_1 x)$. The parameter β is now a free variational quantity. In the variational problem the energy is the sum of the kinetic energy, harmonic potential, and the Coulomb repulsion. For the class of functions (40) we have

$$E_1(\beta)=3\frac{\hbar^2}{m}\beta+\frac{3m\omega_0^2}{8\beta}+\sqrt{\frac{8}{\pi}}\frac{e^2}{4\pi\epsilon}\beta^{1/2}. \qquad (41)$$

The condition for the minimum gives the minimal energy $E_1(\beta_1)$ and the corresponding lengths $\beta_1^{-1/2}$ according to

$$3\frac{\hbar^2}{m}-\frac{3m\omega_0^2}{8\beta_1^2}+\sqrt{\frac{2}{\pi}}\frac{e^2}{4\pi\epsilon}\beta_1^{-1/2}=0. \qquad (42)$$

In the limit where the Coulomb term can be neglected, we find $\beta_1=m\omega_0/(2\sqrt{2}\hbar)$. In the opposite case where the Coulomb part is strong, we have $\beta_1=(\sqrt{\frac{\pi}{2}}\frac{3m\omega_0^2}{8}\frac{4\pi\epsilon}{e^2})^{2/3}$, so that $\beta_1^{-1/2}$ is proportional to x_0 (38). As an interpolating formula we can take

$$\beta_1^{-2}=\frac{8\hbar^2}{m^2\omega_0^2}+\left(\sqrt{\frac{\pi}{2}}\frac{3m\omega_0^2}{8}\frac{4\pi\epsilon}{e^2}\right)^{-4/3}. \qquad (43)$$

A better ansatz for the variational treatment would be the following class of functions

$$\phi_2^{\rm as}(x;\beta,l)=\left(\frac{\beta}{2\pi}\right)^{1/4}\frac{1}{\sqrt{1-e^{-2\beta l^2}}}\times\left[e^{-\beta(x-l)^2}-e^{-\beta(x+l)^2}\right]. \qquad (44)$$

In the limit $l\to 0$ the Hermitian function (40) is recovered. The corresponding energy functional $E_2^{\rm as}(\beta,l)=\langle\phi_2^{\rm as}|H_{\rm rel}|\phi_2^{\rm as}\rangle$ for the Hamiltonian of the relative motion can be also obtained in analytical form but it is not needed here.

With respect to the symmetric solution, we can take $|\phi_1(x;\beta)|$ from Eq. (40) that gives the same energy value as the antisymmetric one. A symmetric wave function $\phi_2^{\rm s}(x;\beta,l)$ that has no nodes can be obtained as symmetric superposition similar to Eq. (44). However, the energy diverges because $\phi_2^{\rm s}(0;\beta,l)\neq 0$. If such singularity of the Coulomb repulsion is removed considering the distribution of the electron wave function in the space as given by the atomic orbits, the symmetric solution may become favorable. For instance, we can replace the Coulomb repulsion by $e^2/(4\pi\epsilon\sqrt{x^2+a^2})$ where a is of the order of the Bohr radius. Then, the degeneration between the symmetric and antisymmetric solution will be removed so that the symmetric solution (spin singlet) becomes energetically favorable. We will come back to this point below when dealing with the Hubbard model.

Instead of the variational approach, the Schrödinger equation (37) for the relative motion can be solved numerically. Potentials for different parameter values of $\bar{\omega}_0$ (in Rydberg units, $\hbar=e^2/(8\pi\epsilon)=2m=1$) are shown in Fig. 2. The corresponding normalized wave functions are also shown in Fig. 2 for $x>0$. For $x<0$ we have the symmetric solution $\phi(-x)=\phi(x)$ and the antisymmetric solution $\phi(-x)=-\phi(x)$ that are degenerated. We see that (40) has the same shape as the numerical solution. However, the harmonic approximation for the deformation potential is justified only near the minimum of the potential, i.e., $x\leqslant a/\kappa$.

To consider also larger values of the relative distance x, we go beyond the harmonic potential by using a soliton

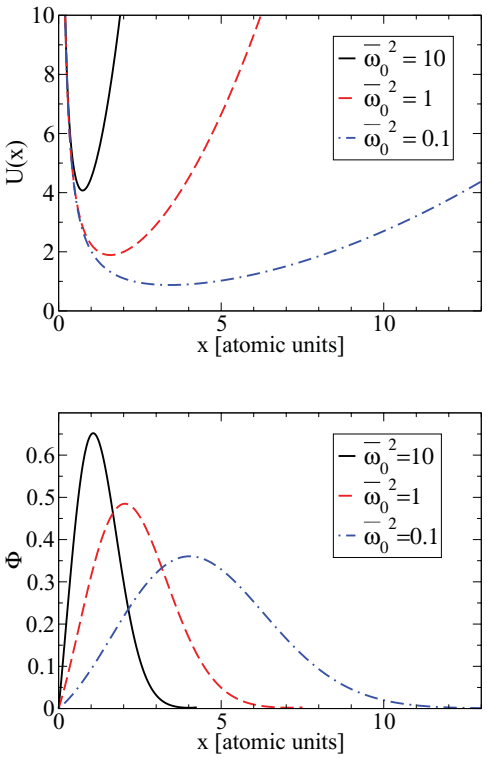

FIG. 2. (Color online) Potential energy of the relative motion (in Rydberg units) and wave function for the relative motion of the electrons from the numerical solution of the Schrödinger equation (37), for different parameter values of $\bar{\omega}_0^2 = m\omega_0^2/\mathrm{Ryd}$.

deformation, and hence we look for solutions of the equation:

$$\left(-\frac{\hbar^2}{ma^2}\frac{d^2}{d\bar{x}^2} - \bar{u}\,\mathrm{sech}^2(\bar{\kappa}\bar{x}) + \frac{e^2}{4\pi\epsilon a|\bar{x}|}\right)\phi(\bar{x}) = E_{\mathrm{rel}}\phi(\bar{x}). \tag{45}$$

The relative distance $\bar{x} = x/a$ is given in units of a. The solution of Eq. (45) indicates the range of parameter values where a bisolectron solution exists. With the parameter values given for polypeptides,[17] we have $\hbar^2/ma^2 \approx 0.2\,\mathrm{eV}, e^2/4\pi\epsilon a \approx 0.5\,\mathrm{eV}$. A bound state exists if $\bar{u}$ exceeds a threshold or critical value $\bar{u}_c$. For instance, we find $\bar{u}_c = 0.4742$ eV for $\bar{\kappa} = 0.3$, $\bar{u}_c = 0.1368$ eV for $\bar{\kappa} = 0.1$. Then $\bar{\kappa} \approx \kappa/\sqrt{2}, \bar{u} \approx \chi a\rho_0$. If we consider the value for $E^{(\mathrm{bind})}$ given at the end of Sec. II to characterize the parameter range of $\bar{u}$, a bisolectron state is stable for values of $\bar{\kappa}$ below the corresponding critical values for polypeptides.

VI. COMPARISON WITH NUMERICAL RESULTS FOR THE HUBBARD MODEL

Let us now compare our analytical results with numerical results of computer simulations using the Hubbard Hamiltonian, for a discrete lattice with Morse interactions[48] (for related works see Refs. 40–43, 47, and 49–52),

$$U^{\mathrm{Morse}}(r) = D[(1 - e^{-B(r-a)})^2 - 1] \tag{46}$$

Having in mind biomolecules we have: lattice spacing $a \simeq 1-5$ Å, lattice stiffness $Ba \simeq 1$, and potential well depth $D \simeq 0.1-0.5$ eV. The period of (linear) oscillations in the Morse well is $1/\Omega_{\mathrm{Morse}} \simeq 0.1-0.5$ ps.

The Morse potential has a repulsive part similar to that of the Toda potential[53] and, for all practical purposes, about the same as that of the Lennard-Jones potential. The attractive component of the Toda interaction is unphysical, which is not significant for our purposes here. Noteworthy is that the Toda lattice Hamiltonian is integrable and we know its exact analytical solution and, besides, we know all its thermodynamic quantities in compact analytical form. Furthermore, exploring numerically the Morse Hamiltonian dynamics it has been found that there is no significant difference between the results found for the Toda and the Morse lattices.[24,53–55] Accordingly, we will benefit from this in our computations here.[24,54–56] Note also that the potential energy of a lattice with Morse interaction can be expanded in a power series with respect to the displacements of the atoms from equilibrium positions thus leading to the cubic term earlier used in our analytical approach.

The electron part using the Hubbard Hamiltonian (2) and (5), is

$$H_{\mathrm{el}} + H_{\mathrm{Coul}} = -\sum_{n,s} J_{n,n+1}(\hat{c}^\dagger_{n+1s}\hat{c}_{ns} + \hat{c}^\dagger_{ns}\hat{c}_{n+1s}) + U\sum_n \hat{c}^\dagger_{n\uparrow}\hat{c}^\dagger_{n\downarrow}\hat{c}_{n\downarrow}\hat{c}_{n\uparrow}. \tag{47}$$

where $U_{n,m} = U\delta_{n,m}$ is a local form of Coulomb repulsion. The quantities $J_{n,n+1}$ denote the transfer matrix elements whose value are determined by an overlap integral being responsible for the nearest-neighbor transport of the electron along the lattice. Following Slater,[57] these transfer matrix elements depend on the relative distance between two consecutive units in the following exponential fashion:

$$J_{n,n+1} = J_0 \exp[-\eta(u_{n+1} - u_n)]. \tag{48}$$

The quantity η regulates how strong the $J_{n,n+1}$ are influenced by the relative displacement of lattice units, or in other words it determines the coupling strength between the electron and the lattice system. The numerical methods to solve the Hubbard model system coupled to the Morse lattice are given in Refs. 42 and 58.

We will use the comparison with the Hubbard model to assess the validity of the approximations used above. In particular, the transition to the continuum limit is possible when the relevant properties vary smoothly in the lattice. With respect to the Coulomb interaction this means that the characteristic length scale given here by the width of the bisolectron $2\pi a/\kappa$ is large compared with the lattice parameter a. In the opposite case, the Coulomb interaction singular at $x = 0$ cannot be used. A Hubbard Hamiltonian, in general with two-center Coulomb repulsion terms, may become more appropriate.

The numerical results for electron pairs with (local) single-site Hubbard repulsion are shown in Fig. 3 for the electron pair density (blue solid line) and the particle velocity distribution (red dashed line). The parameter values used in the computer simulations are: $\eta = 2.5a, J_0 = 0.04D$. The adiabaticity parameter $\tau = J_0/(\hbar\Omega_{\mathrm{Morse}})$ was fixed at $\tau = 20$. The Hubbard parameter, U, was also measured in units of the oscillation

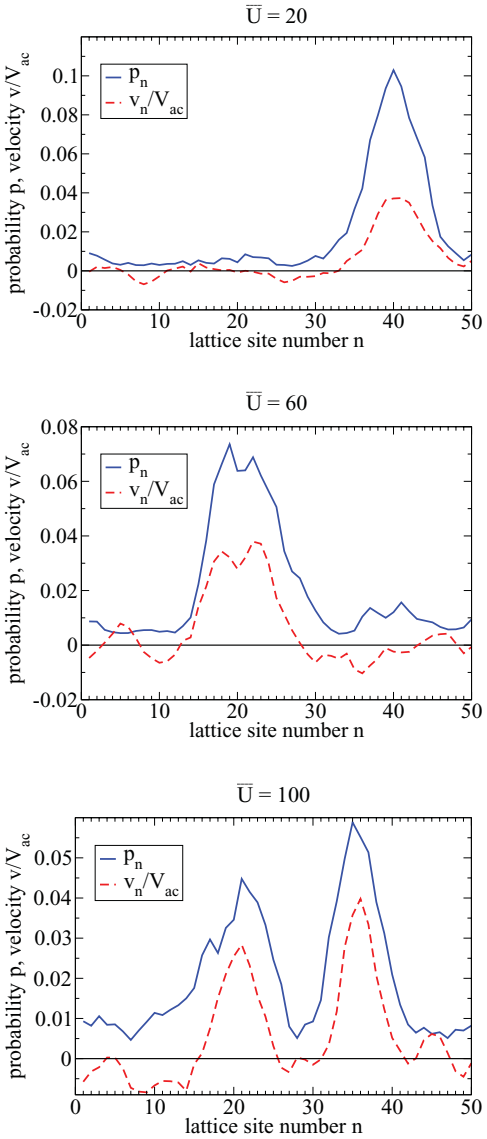

FIG. 3. (Color online) Numerical estimates for the electron density (blue solid line) and the velocity distribution (red dashed line) of solectron pairs with Hubbard repulsion at $\bar{U} = 20,60,100$ on the Morse lattice.

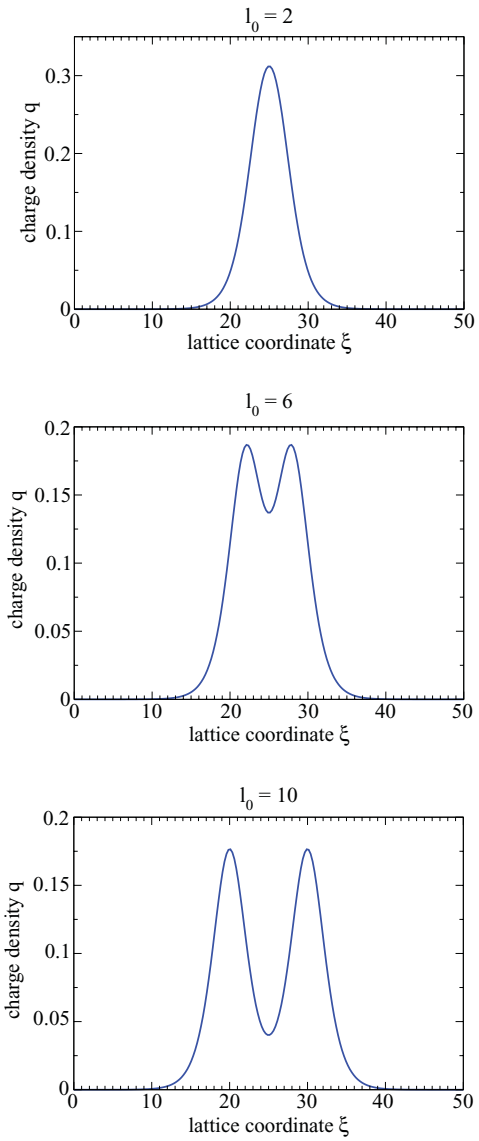

FIG. 4. (Color online) Estimates of the bisolectron charge density profile $q(\xi)$, vs. the lattice coordinate ξ using the analytical result (22) with $\gamma = 1.5$, $\kappa = 0.35$, and $l_0 = 2,6,10$.

energy of the Morse potential with $\bar{U} = U/\hbar\Omega_{\text{Morse}}$. For illustration, we took: $\bar{U} = 20,60,100$. Furthermore, $\hbar\Omega_{\text{Morse}} = 0.002D$. With values of the depth of the potential well in the range of $D \simeq 0.1$–0.5 eV, we see that the lowest $\bar{U} = 20$ would correspond to $U = 0.004$–0.02 eV and the highest $\bar{U} = 100$ would correspond to $U = 0.02$–0.1 eV. Coulomb repulsion energies in this range is what one expects from physical estimates for electron pairs in a medium with a relative dielectric constant $\epsilon_{\text{rel}} \simeq 10$. Thus Hubbard parameter values in the range $\bar{U} = 20$–100 correspond to Coulomb repulsion energies in the range $U \simeq 0.01$–0.05 eV.

Figure 3 shows that depending on the repulsion there can be one or two peaks in both characteristics, the probability distribution and the velocity distribution. The probability distribution gives the probability to find an electron at a given lattice point, independent on the lattice position of the other electron. It measures the electron density. The velocity distribution indicates that there is a collective flow as expected for a solitonlike excitation.

In Fig. 4 we show the charge density function obtained above in Sec. III, for various values of the Coulomb repulsion, which determines the distance between the maxima of one-electron functions. The charge density is determined by Eq. (24) with $l = l_0$ (27). This allows us to place in parallel 2, 6, and 10 for l_0 in the three Figs. 4 with 20, 60, and 100 for $\tilde{U}$ in Fig. 3. We cannot expect a one-to-one correspondence between the numerical and analytical results. However, we see quite a good qualitative agreement between the results of the two approaches. In particular, we see that electrons are localized in the bisolectron state, whose profile depends on the strength of the Coulomb repulsion. The tendency that one maximum splits into two maxima with increasing Coulomb repulsion is also clearly seen in both approaches.

It clearly appears in Figs. 3 and 4 that increasing the Hubbard parameter U has a similar effect as increasing

the distance parameter in the analytical theory (Sec. II) or otherwise said increasing the Coulomb repulsion strength, Eq. (29). Both effects push the centers of the wave functions to go away from each other. The parameter values used in the computer simulations, correspond to relatively high nonadiabaticity of the system and strong anharmonicity. Nevertheless, comparison of the three sets of figures corresponding to three different values of the Hubbard term in numerical simulations and Coulomb term in the analytical model shows that our analytical model gives rather good results even for rather strong electron repulsion. The approximations performed in deriving our analytical model, in particular the transition to the continuum description and the expansions in deriving the nonlinear potential and the separation of the center of mass motion from the relative motion, seem not to alter significantly the qualitative behavior of the bisolectron solution in the parameter range considered here.

VII. CONCLUSIONS

We have shown that the anharmonicity of a lattice favors electron pairing in lattice solitonlike deformation wells. In the particular case of *cubic* anharmonicity, explicit expressions for the electron wave function and the traveling lattice deformation have been found. We have also given here the first excited state, which is a triplet state of two electrons with parallel spins with antisymmetric spatial wave function. We find also limits of the continuum description if the relative distance between the electrons becomes comparable with the lattice parameter for strongly localized electrons. Then, the singular Coulomb interaction ($\propto 1/|x|$) should be replaced by the matrix elements with respect to the tight-binding orbitals, and higher-order derivatives in the continuum approximation should be taken into account.

The bisolectron found here (a soliton binding two electrons with Coulomb repulsion and Pauli's principle incorporated), can move with velocity up to the sound velocity, with energy and momentum, maintaining finite values also at the sound velocity. Low-dimensional systems, mentioned in the Introduction, are characterized by parameter values, for which the adiabatic approximation is valid. Their ground electron state is a solectron (a bound electron to a soliton) extends over a few lattice sites. Therefore, we expect that in these systems pairing of electrons takes place at enough level of doping.

Comparison of the energy of such a bisolectron with the energy of the two independent solitons binding a single electron each (two separate solectrons) shows that there is gain of energy even including the Coulomb repulsion. For illustration we have estimated the bisolectron binding energy for parameter values typical for biological macromolecules (poly-peptides). In conclusion, lattice *anharmonicity*, leading to lattice solitonlike deformations, enhances pairing of electrons, or, in other words, strong electron correlation both in *momentum* space and in *real* space. Such a conclusion is of "universal" value as there is quite a good qualitative agreement between the results from an analytical model for two electrons in a singlet bisolectron state with account of Coulomb repulsion, and the numerical results from computer simulations using the Hubbard (local) model.

ACKNOWLEDGMENTS

The authors are grateful to A.S. Alexandrov, E. Brändäs, L. Cruzeiro, F. de Moura, J. Feder, R. Lima, G. Vinogradov, and E.G. Wilson for enlightening discussions and/or correspondence. This research was supported by the Spanish Ministerio de Ciencia e Innovacion under Grant Nos. EXPLORA FIS2009-06585 and MAT2011-26221. L. Brizhik acknowledges partial support from the Fundamental Research Grant of the National Academy of Sciences of Ukraine.

[1] E. G. Wilson, J. Phys. C: Solid State Phys. **16**, 6739 (1983).
[2] K. J. Donovan and E. G. Wilson, Philos. Mag. B **44**, 9 (1981); **44**, 31 (1981).
[3] K. J. Donovan and E. G. Wilson, J. Phys. C: Solid State Phys. **18**, L-51 (1985).
[4] A. S. Gogolin, JETP Lett. **43**, 511 (1986); Phys. Rep. **157**, 347 (1988), and references therein.
[5] *Electronic Properties of Inorganic Quasi-One-Dimensional Compounds*, Part II, edited by P. Monceau (Reidel, Dordrecht, 1985).
[6] B. G. Streetman and S. K. Banerjee, *Solid State Electronic Devices* (Prentice-Hall, Upper Saddle River, NJ, 2009).
[7] Y. Zhang, X. Ke, C. Chen, J. Yang, and P. R. C. Kent, Phys. Rev. B **80**, 024304 (2009).
[8] *PdO Crystal Structure, Lattice Parameters, Thermal Expansion, Vol. 41D: Non-Tetrahedrally Bonded elements and Binary Compounds I*, edited by O. Madelung, U. Rössler, and M. Schultz (Springer, Berlin, 1998).
[9] J. Androulakis, Y. Lee, I. Todorov, D.-Y. Chung, and M. Kanatzidis, Phys. Rev. B **83**, 195209 (2011).
[10] C. Falter and G. A. Hoffmann, Phys. Rev. B **64**, 054516 (2001).
[11] K.-P. Bohnen, R. Heid, and M. Krauss, Europhys. Lett. **64**, 104 (2003).
[12] T. P. Devereaux, T. Cuk, Z.-X. Shen, and N. Nagaosa, Phys. Rev. Lett. **93**, 117004 (2004).
[13] D. Reznik, L. Pintschovius, M. Ito, S. Iikubo, M. Sato, H. Goka, M. Fujita, K. Yamada, G. D. Gu, and J. M. Tranquada, Nature (London) **440**, 1170 (2006).
[14] V. Z. Kresin and S. A. Wolf, Rev. Mod. Phys. **81**, 481 (2009).
[15] D. M. Newns and C. C. Tsuei, Nat. Phys. **3**, 184 (2007).
[16] A. S. Davydov, *Solitons in Molecular Systems* (Reidel, Dordrecht, 1991).
[17] A. C. Scott, Phys. Rep. **217**, 1 (1992).
[18] *Davydov's Soliton Revisited. Self-trapping of Vibrational Energy in Protein*, edited by P. L. Christiansen and A. C. Scott (Plenum, New York, 1990).
[19] *Proton Transfer in Hydrogen-Bonded Systems*, edited by T. Bountis (Plenum, New York, 1992).
[20] T. Dauxois and M. Peyrard, *Physics of Solitons* (Cambridge University Press, Cambridge, 2006).

[21]L. V. Yakushevich, *Nonlinear Physics of DNA* (Wiley-VCH, Weinheim, 2004).
[22]M. Peyrard and J. Farago, Physica A **288**, 199 (2000).
[23]L. I. Manevich and V. V. Simmons, *Solitons in Macromolecular Systems* (Nova, New York, 2008).
[24]M. G. Velarde, J. Comput. Appl. Math. **233**, 1432 (2010).
[25]L. D. Landau, Phys. Z. Sowjetunion **3**, 664 (1933).
[26]S. I. Pekar, *Untersuchungen über die Elektronentheorie* (Akademie Verlag, Berlin, 1954).
[27]M. I. Kaganov and I. M. Lifshitz, *Quasiparticles* (Mir, Moscow, 1979).
[28]A. S. Alexandrov and N. Mott, *Polarons and Bipolarons* (World Scientific, Cambridge, 1995).
[29]*Polarons in Advanced Materials*, edited by A. S. Alexandrov (Springer, Dordrecht, 2007).
[30]A. S. Alexandrov and J. T. Devreese, *Advances in Polaron Physics* (Springer, Dordrecht, 2009).
[31]*Polarons in Ionic Crystals and Polar Semiconductors*, edited by J. T. Devreese (North-Holland, Amsterdam, 1972).
[32]A. S. Davydov and A. V. Zolotaryuk, Phys. Lett. **94**, 49 (1983).
[33]A. S. Davydov and A. V. Zolotaryuk, Phys. Status Solidi B **115**, 115 (1983).
[34]A. S. Davydov and A. V. Zolotaryuk, Phys. Scr. **30**, 426 (1984).
[35]L. S. Brizhik and A. S. Davydov, J. Low Temp. Phys. **10**, 748 (1984).
[36]L. S. Brizhik, J. Low Temp. Phys. **12**, 437 (1986).
[37]L. S. Brizhik and A. A. Eremko, Physica D **81**, 295 (1995).
[38]M. G. Velarde, L. Brizhik, A. P. Chetverikov, L. Cruzeiro, W. Ebeling, and G. Röpke, Int. J. Quantum Chem. **112**, 551 (2012).
[39]M. G. Velarde, L. Brizhik, A. P. Chetverikov, L. Cruzeiro, W. Ebeling, and G. Röpke, Int. J. Quantum Chem. **112**, 2591 (2012).
[40]D. Hennig, M. G. Velarde, W. Ebeling, and A. P. Chetverikov, Phys. Rev. E **78**, 066606 (2008).
[41]W. Ebeling, M. G. Velarde, A. P. Chetverikov, and D. Henning, in *Selforganization of Molecular Systems. From Molecules and Clusters to Nanotubes and Proteins*, edited by N. Russo, V. Ya. Antonchenko, and E. Kryachko (Springer, Berlin 2009), pp. 171–198.
[42]M. G. Velarde, W. Ebeling, and A. P. Chetverikov, Int. J. Bifurcation Chaos **21**, 1595 (2011).
[43]M. G. Velarde and C. Neissner, Int. J. Bifurcation Chaos **18**, 885 (2008).
[44]*The Hubbard Model. A Reprint Volume*, edited by A. Montorsi (World Scientific, Singapore, 1992).
[45]J. Hubbard, Proc. R. Soc. London A **276**, 238 (1963); **277**, 237 (1964); **281**, 401 (1964).
[46]A. V. Zolotaryuk, K. H. Spatschek, and A. V. Savin, Phys. Rev. B **54**, 266 (1996).
[47]W. S. Dias, M. L. Lyra, and F. A. B. F. de Moura, Eur. Phys. J. B **85**, 7 (2012).
[48]P. Morse, Phys. Rev. **34**, 57 (1929).
[49]L. Cruzeiro, J. C. Eilbeck, J. L. Marin, and F. M. Russell, Eur. Phys. J. B **42**, 95 (2004).
[50]A. P. Chetverikov, W. Ebeling, and M. G. Velarde, Eur. Phys. J. B **70**, 217 (2009).
[51]W. S. Dias, M. L. Lyra, and F. A. B. F. de Moura, Phys. Lett. A **374**, 4554 (2010).
[52]W. S. Dias, E. M. Nascimento, M. L. Lyra, and F. A. B. F. de Moura, Phys. Rev. B **81**, 045116 (2010).
[53]M. Toda, *Theory of Nonlinear Lattices*, 2nd ed. (Springer, Berlin, 1989).
[54]J. Dancz and S. A. Rice, J. Chem. Phys. **67**, 1418 (1977).
[55]T. J. Rolfe, S. A. Rice, and J. Dancz, J. Chem. Phys. **79**, 26 (1979).
[56]A. P. Chetverikov, W. Ebeling, and M. G. Velarde, Eur. Phys. J. B **51**, 87 (2006).
[57]J. C. Slater, *Quantum Theory of Molecules and Solids*, Vol. 4 (McGraw-Hill, New York, 1974).
[58]W. Ebeling, M. G. Velarde, and A. P. Chetverikov, Condens. Matter Phys. **12**, 633 (2009).